Quantum theory of noise in phase conjugation by four-wave mixing in a two-level system

R. W. Schirmer,* M. Y. Lanzerotti,* and A. L. Gaeta
School of Applied and Engineering Physics, Cornell University, Ithaca, New York 14853

G. S. Agarwal
Physical Research Laboratory, Navrangpura, Ahmedabad, 380 009, India
(Received 7 October 1996)

A quantum theory of nearly degenerate backward four-wave mixing in a two-level atomic system is developed. The theory is used to calculate the quantum noise produced by a phase-conjugate mirror based on this system. The results indicate that in the case of pure radiative broadening the ideal quantum-noise limit is reached for relatively small pump-wave strengths and for relatively large probe-pump and pump-resonance detunings, so that the phase-conjugate reflectivity is far from its maximum value. Conversely, in the collisionally broadened case, operation closest to the quantum-noise limit occurs near the point of maximum reflectivity. [S1050-2947(97)03604-4]

PACS number(s): 42.50.Lc, 42.65.Hw

I. INTRODUCTION

Phase conjugation is an optical process that has drawn interest because of its applications in aberration correction and image processing [1,2], laser-linewidth reduction [3], and correcting for the effects of dispersion and nonlinearity in optical fibers [4–6]. A phase-conjugate mirror (PCM) is a type of optical amplifier that generates the counterpropagating phase conjugate of an input signal field. It can be shown that any phase-conjugating optical amplifier is required by quantum mechanics to introduce a minimum amount of noise into the conjugate field [7,8]. In practice, a PCM operates above this ideal quantum-noise limit (i.e., introduces noise in excess of the required minimum amount), and the generated noise spectrum depends on the nonlinear mechanism used to produce the conjugate field. The noise generated by a PCM impacts on its ability to perform functions such as aberration correction and the conjugation of nonclassical (e.g., squeezed) states of light [9,10]. Furthermore, the noise is predicted to play a role in the dynamics of atoms placed in front of the PCM [11].

Four-wave mixing is one of the standard techniques used to perform phase conjugation and has been demonstrated in atomic vapors [12–17], photorefractive materials [18–20], Brillouin-active media [21–23], and semiconductor diode amplifiers [5,6,24]. The noise produced in four-wave mixing (for both backward and forward geometries) has been studied theoretically by a number of researchers. Yuen and Shapiro [25], Jansky and Yushin [26], and Yurke [27] all treated squeezing via backward four-wave mixing with undepleted classical pump fields in a nonlinear medium characterized by phenomenological coupling constants. The effects of pump quantization have also been included in four-wave mixing models [28,29], and Bondurant *et al.* [28] examined the effects of pump absorption. In these studies the nonlinear medium was treated phenomenologically. Agarwal [30] and Sargent, Holm, and Zubairy [31] all developed general formalisms for treating nonlinear wave mixing in an atomic system. Agarwal and Boyd [32] treated Rabi sideband generation by forward four-wave mixing for the specific case of a two-level system. Levenson *et al.* [33] studied the noise generated by forward four-wave mixing in an optical fiber. Reid and Walls [34–36] analyzed degenerate four-wave mixing (both backward and forward geometries) in a two-level system, and nearly degenerate forward four-wave mixing in a two-level system placed in a cavity. In both cases classical, undepleted pump waves were assumed and attention was concentrated on the radiatively broadened limit. Ho, Kumar, and Shapiro [37] developed a theory for nondegenerate forward four-wave mixing in a two-level system which included the effects of collisions, probe-pump phase mismatch, Doppler broadening, and Gaussian beam profiles. Experimental measurements of the noise generated in four-wave mixing have also been made. Slusher *et al.* [38] measured the noise generated by four-wave mixing in a sodium beam within an optical cavity and achieved 20% squeezing. Shelby *et al.* [39] measured the quadrature noise generated by forward four-wave mixing in an optical fiber and achieved 12% squeezing. Bespalov Matreev, and Pasmanik [21] studied the noise properties of a PCM based on Brillouin-enhanced four-wave mixing (BEFWM) and conjugated pulses with energies as small as 10^{-11} J at a signal-to-noise ratio (SNR) of 1:1. Andreev *et al.* [22] used a laser preamplifier at the input of a BEFWM-PCM to conjugate pulses with energies as small as 4×10^{-17} J at a SNR of 6:1. Ridley and Scott [23] used a PCM based on stimulated Brillouin scattering with a Brillouin preamplifier to conjugate pulses with energies as small as 3×10^{-13} J at a SNR of 10:1.

In this paper, we give a quantum-mechanical treatment of phase conjugation by nearly degenerate backward four-wave mixing in a two-level system. The atomic response is treated to first order in the quantized signal and conjugate fields and to all orders in the classical, nondepleted pump waves. The dephasing effects of collisions are included in the model, but other effects of atomic motion (i.e., Doppler broadening and grating wash-out) are not. We calculate the spectrum of the

*Permanent address: Department of Physics, Cornell University, Ithaca, NY 14853.

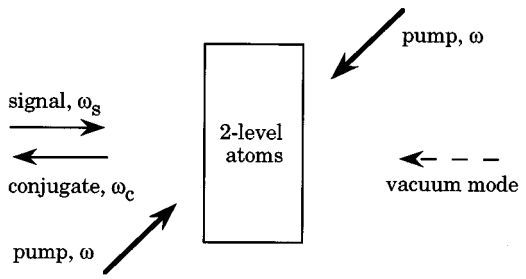

FIG. 1. Backward four-wave mixing geometry.

conjugate beam and the phase-conjugate reflectivity R_{pc} of the PCM for a range of conditions, including both the radiatively broadened and nonradiatively broadened limits. This information is used to calculate the photon noise factor, a quantity which measures the PCM's noise performance relative to the ideal quantum-noise limit. We find that the conditions that maximize R_{pc} are also the conditions under which the atomic fluctuations contribute a significant amount of excess noise to the conjugate field. For the case of pure radiative broadening, this excess noise causes the PCM to operate farthest from the ideal quantum-noise limit in the regime where R_{pc} is near maximum. Conversely, in the case in which the atoms are collisionally broadened, the PCM operates closest to the quantum-noise limit in the regime where R_{pc} is near maximum. Our work is motivated primarily by recent experimental studies of the noise generated by a continuous-wave potassium-vapor based PCM and by efforts to use it to perform phase conjugation and aberration correction with very low signal beam powers [40,41].

II. QUANTUM THEORY

The theory of phase conjugation in a two-level system can be formulated using the general quantum-mechanical theory of multiwave mixing presented by Agarwal [30]. Previous studies of the spectra produced via wave mixing in two-level systems using this technique include theoretical analyses of forward four-wave mixing [32], signal amplification by two-beam coupling [42], noise generation in two-beam coupling in the presence of Doppler broadening [43], and a theoretical and experimental investigation of the noise acquired by a single, strong beam passing through a potassium vapor [44]. Figure 1 shows the backward four-wave mixing geometry. Two strong pump beams of frequency ω interact with a signal field of frequency ω_s in a two-level medium with resonance frequency ω_0 to produce a conjugate field at frequency ω_c. The Hamiltonian for the total system is given by

$$\hat{H}=\hat{H}_A+\hat{H}_F+\hat{H}_I, \tag{2.1}$$

where $\hat{H}_A$ and $\hat{H}_F$ are the unperturbed Hamiltonians for the collection of two-level atoms and the electromagnetic field, respectively. In the electric-dipole approximation, the interaction Hamiltonian $\hat{H}_I$ is given by

$$\hat{H}_I=-\int d^3r\hat{\mathbf{P}}(\mathbf{r},t)\cdot\hat{\mathbf{E}}(\mathbf{r},t), \tag{2.2}$$

where $\hat{\mathbf{P}}(\mathbf{r},t)$ is the polarization operator and $\hat{\mathbf{E}}(\mathbf{r},t)$ is the total electric-field operator. The electric field is composed of the signal field, the conjugate field, and the two counterpropagating pump fields, such that

$$\hat{\mathbf{E}}(\mathbf{r},t)=\hat{\mathbf{E}}_s(\mathbf{r},t)+\hat{\mathbf{E}}_c(\mathbf{r},t)+\mathbf{E}_p(\mathbf{r},t). \tag{2.3}$$

The total pump field is given by

$$\mathbf{E}_p(\mathbf{r},t)=\mathbf{A}_p[e^{i(\mathbf{k}\cdot\mathbf{r}-\omega t)}+e^{-i(\mathbf{k}\cdot\mathbf{r}+\omega t)}]+\text{c.c.}, \tag{2.4}$$

where both pump waves are assumed to have the same amplitude and are treated classically. The signal field operator is given by

$$\hat{\mathbf{E}}_s(\mathbf{r},t)=\beta_s\boldsymbol{\epsilon}_s\hat{a}_s e^{i(\mathbf{k}_s\cdot\mathbf{r}-\omega_s t)}+\text{H.c.}, \tag{2.5}$$

and the conjugate field operator is given by

$$\hat{\mathbf{E}}_c(\mathbf{r},t)=\beta_c\boldsymbol{\epsilon}_c\hat{a}_c e^{i(\mathbf{k}_c\cdot\mathbf{r}-\omega_c t)}+\text{H.c.}, \tag{2.6}$$

where $\hat{a}_i$ for $i=(s,c)$ is the photon annihilation operator, $\beta_i=-i(2\pi\hbar\omega_i/V)^{1/2}$, $\boldsymbol{\epsilon}_i$ is the polarization unit vector (all waves are taken to have the same polarization), ω_i is the mode frequency, and V is the quantization volume. The signal and conjugate frequencies are related by $\omega_c=2\omega-\omega_s$. The polarization operator for the collection of two-level atoms is given by

$$\hat{\mathbf{P}}(\mathbf{r})=\sum_i \mu_i\delta(\mathbf{r}-\mathbf{R}_i)\hat{S}^+ +\text{H.c.}, \tag{2.7}$$

where $\mathbf{R}_i$ is the position of atom i, μ_i is its dipole matrix element, and its harmonic time dependence has been suppressed. The operator $\hat{S}^+$, its Hermitian conjugate $\hat{S}^-$, and $\hat{S}^z=[\hat{S}^+,\hat{S}^-]/2$ obey the commutation relations for a spin-1/2 system. It is assumed that the frequencies of the signal and conjugate waves are sufficiently close to the atomic resonance at frequency ω_0 that the rotating-wave approximation can be made. The interaction Hamiltonian then becomes

$$\hat{H}_I=-\int d^3r\hat{\mathbf{P}}^-(\mathbf{r},t)\cdot[\mathbf{E}_p^+(\mathbf{r},t)+\hat{\mathbf{E}}_s^+(\mathbf{r},t)+\hat{\mathbf{E}}_c^+(\mathbf{r},t)]+\text{H.c.}, \tag{2.8}$$

where the superscripts $(+)$ and $(-)$ denote the positive- and negative-frequency components of the field, respectively.

The density operator for the coupled atom-field system $\hat{\rho}$ obeys the equation of motion

$$\frac{\partial\hat{\rho}}{\partial t}=\frac{-i}{\hbar}[\hat{H}_A+\hat{H}_F+\hat{H}_I,\hat{\rho}]+\left(\frac{\partial\hat{\rho}}{\partial t}\right)_{relax}. \tag{2.9}$$

The relaxation term in Eq. (2.9),

$$\left(\frac{\partial\hat{\rho}}{\partial t}\right)_{relax}=\begin{bmatrix}\rho_{22}/T_1 & -\rho_{12}/T_2\\ -\rho_{21}/T_2 & -\rho_{22}/T_1\end{bmatrix}, \tag{2.10}$$

includes the contributions of spontaneous emission and elastic dephasing processes. By substituting Eqs. (2.4)–(2.8) into Eq. (2.9), the polarization is calculated to first order in the

signal and conjugate fields, and to all orders in the pump fields. Using this expression for the polarization as the source term in the quantized Maxwell equations and making the slowly varying-envelope approximation, the equations governing the evolution of the signal- and conjugate-field operators are found to be

$$\frac{d\hat{a}_s}{dz}=\alpha_1\hat{a}_s+i\kappa_1^*\hat{a}_c^\dagger+\hat{L}_1 \tag{2.11}$$

and

$$\frac{d\hat{a}_c^\dagger}{dz}=-\alpha_2\hat{a}_c^\dagger+i\kappa_2\hat{a}_s+\hat{L}_2. \tag{2.12}$$

The propagation coefficients α and κ are the same as those obtained from a semiclassical treatment of phase conjugation in a two-level system [45] and represent the mean response of the atomic medium. Their explicit forms are given in Appendix A. The Langevin noise operators $\hat{L}_1$ and $\hat{L}_2$ are proportional to the deviation of the polarization from its mean value and account for the effects of fluctuations in the atomic medium. The moments of the noise operators may be written as

$$\langle L_1(z)L_1^\dagger(z')\rangle=\alpha_0\delta(z-z')\widetilde{X}^{-+}(\delta_s), \tag{2.13a}$$

$$\langle L_2(z)L_2^\dagger(z')\rangle=\alpha_0\delta(z-z')\widetilde{X}^{+-}(\delta_s), \tag{2.13b}$$

and

$$\langle L_2(z)L_1^\dagger(z')\rangle=\alpha_0\delta(z-z')\widetilde{X}^{++}(\delta_s), \tag{2.13c}$$

where

$$\widetilde{X}^{-+}(\delta_s)=\frac{1}{2\pi}\int d\tau\, e^{-i\delta_s\tau}\lim_{t\to\infty}[\langle\hat{S}^-(t)\hat{S}^+(t+\tau)\rangle -\langle\hat{S}^-(t)\rangle\langle\hat{S}^+(t+\tau)\rangle], \tag{2.14a}$$

$$\widetilde{X}^{+-}(\delta_s)=\frac{1}{2\pi}\int d\tau\, e^{-i\delta_s\tau}\lim_{t\to\infty}[\langle\hat{S}^+(t)\hat{S}^-(t+\tau)\rangle -\langle\hat{S}^+(t)\rangle\langle\hat{S}^-(t+\tau)\rangle], \tag{2.14b}$$

and

$$\widetilde{X}^{++}(\delta_s)=\frac{1}{2\pi}\int d\tau\, e^{-i\delta_s\tau}\lim_{t\to\infty}[\langle\hat{S}^+(t)\hat{S}^+(t+\tau)\rangle -\langle\hat{S}^+(t)\rangle\langle\hat{S}^+(t+\tau)\rangle]. \tag{2.14c}$$

Here $\alpha_0=4\pi\mu^2N\omega T_2/\hbar c$ is the small-signal, line-center absorption coefficient, N is the density of atoms, and $\delta_s=\omega_s-\omega$ is the probe-pump detuning. The right-hand sides of Eqs. (2.14a)–(2.14c) have been averaged over a spatial period of the grating created by the counterpropagating pump waves to eliminate non-phase-matched terms. We assume that the fluctuations in the polarizations of different atoms are uncorrelated, which results in the moments of the noise operators being δ correlated in z [i.e., $\delta(z-z')$]. By introducing the propagation matrix K, where

$$K=\begin{bmatrix}\alpha_1 & i\kappa_1^*\\ i\kappa_2 & -\alpha_2\end{bmatrix}, \tag{2.15}$$

and the two vectors

$$\Psi=\begin{bmatrix}\hat{a}_s\\ \hat{a}_c^\dagger\end{bmatrix} \tag{2.16}$$

and

$$L=\begin{bmatrix}\hat{L}_1\\ \hat{L}_2\end{bmatrix}. \tag{2.17}$$

Equations (2.11) and (2.12) may be rewritten as

$$\frac{d\Psi}{dz}=K\Psi+L. \tag{2.18}$$

Integration of Eq. (2.18) gives the general solution

$$\Psi(z)=e^{Kz}\Psi(0)+\int_0^z d\xi\, e^{K(z-\xi)}L(\xi). \tag{2.19}$$

We take the conjugate field at $z=L$ (where L is the length of the medium) to be in a vacuum state and use Eq. (2.19) to calculate the output conjugate field at $z=0$. Using $[\hat{a}_s,\hat{a}_s^\dagger]=1$, the photon-number spectrum $n_c(\delta_s)$ for the output conjugate field at $z=0$ is found to be

$$n_c(\delta_s)=\langle\hat{a}_c^\dagger\hat{a}_c\rangle=R_{pc}(\delta_s)n_s(\delta_s)+R_{pc}(\delta_s)+N_n(\delta_s), \tag{2.20}$$

where $n_s(\delta_s)=\langle\hat{a}_s^\dagger\hat{a}_s\rangle$ is the input photon number at $z=0$, the phase-conjugate reflectivity is given by $R_{pc}(\delta_s)=|M_{21}(L)|^2/|M_{22}(L)|^2$, M_{ij} are the elements of the matrix $M=\exp(Kz)$, and the excess noise $N_n(\delta_s)$ is given by

$$N_n(\delta_s)=\frac{\alpha_0}{|M_{22}(L)|^2}\int_0^L d\xi[|M_{21}(\xi)|^2\widetilde{X}^{-+}(\delta_s) +|M_{22}(\xi)|^2\widetilde{X}^{+-}(\delta_s)+\{M_{21}^*(\xi)M_{22}(\xi)\widetilde{X}^{++}(\delta_s) +\text{c. c.}\}]. \tag{2.21}$$

The first term on the right-hand side of Eq. (2.20) represents the conjugate-reflected input signal photons. The second term results from the noncommutative nature of the annihilation and creation operators and represents the inherent quantum noise introduced by the phase-conjugation process, even in the case of a nonlinear medium that does not undergo any real excitation [9]. The third term represents noise in excess of the required minimum amount that results from spontaneous emission and collisions in the medium.

The expressions [(2.14a)–(2.14c)] for the polarization correlation functions that appear in Eq. (2.21) are evaluated by solving the optical Bloch equations in steady state for a two-level atom in the presence of the pump fields. It is sufficient to solve the semiclassical Bloch equations in the ab-

sence of the probe and conjugate fields in order to obtain the field evolution equations (2.11) and (2.12) to first order in the probe and conjugate fields. A summary of this calculation is given in Appendix B.

Since the minimum number of noise photons produced by an ideal PCM at frequency δ_s is equal to $R_{pc}(\delta_s)$, we introduce a photon-noise factor

$$N_{ph}(\delta_s)=1+\frac{N_n(\delta_s)}{R_{pc}(\delta_s)}, \tag{2.22}$$

which compares the total noise generated by the PCM to that which would be generated by an ideal quantum-noise limited PCM of the same reflectivity. We define the ideal quantum-noise limit to be the case where $N_{ph}=1$. Note that N_{ph} also measures the strength of the total generated noise relative to the gain of the four-wave mixing process (i.e., R_{pc}). Therefore, minimizing N_{ph} corresponds to maximizing the gain of the PCM relative to the noise it produces.

III. NUMERICAL RESULTS

We examine the noise properties of this system by numerically evaluating the expressions for the reflectivity and photon-noise factor derived in Sec. II. The normalized model parameters upon which the reflectivity and photon-noise factor depend are the absorption path length $\alpha_0 L$, the decay time ratio T_2/T_1, the probe-pump detuning $\delta_s T_2$, the pump-resonance detuning ΔT_2, and the pump strength $\Omega_0 T_2$, where $\Delta=\omega-\omega_0$ and $\Omega_0=4\mu|\mathbf{A}_p|/\hbar$ is the on-resonance Rabi frequency of the total pump field. Since we do not treat the effects of pump absorption, the model is expected to be most accurate for $\alpha_0 L/[1+(\Delta T_2)^2+\Omega_0^2 T_1 T_2]<1$ where the effects of pump absorption are less significant.

We first maximize the reflectivity by varying the pump-resonance detuning and pump strength while holding the probe-pump detuning and the absorption path length fixed. The behavior of the maximum reflectivity is examined as a function of the ratio T_2/T_1 (see Fig. 2). The pump-resonance detuning and pump strength are selected for optimization because they are typically adjusted in actual experiments to achieve the maximum reflectivity. We hold the absorption path length fixed since, in the absence of pump absorption in the model, larger values of $\alpha_0 L$ always yield larger reflectivities. The probe-pump detuning is held fixed at a nonzero value, despite the fact that the maximum reflectivity typically occurs at $\delta_s T_2=0$, because in any experiment the classical noise of the pump waves will dominate all other noise sources at the degenerate frequency. Figure 2(a) shows the maximum reflectivity as a function of the ratio $T_2/2T_1$ for $\delta_s T_2=5$ and $\alpha_0 L=40$, 2, and 0.2. The plot demonstrates that the maximum reflectivity drops with increasing collisions and decreasing $\alpha_0 L$. Figures 2(b) and 2(c) show the values of ΔT_2 and $\Omega_0 T_2$, respectively, that produce the reflectivity curves shown in Fig. 2(a). The optimized values of these two parameters are changing in such a way that the Rabi sidebands ($\delta_{Rabi}^2=\Omega_0^2+\Delta^2$) remain at $\delta_{Rabi}T_2\sim 5$ over the full range of T_2/T_1, near where the signal beam is tuned. Figure 2(d) shows the corresponding photon-noise factor curves and indicates that N_{ph} increases as T_2/T_1 decreases. This result is expected, since decreasing T_2/T_1 increases the

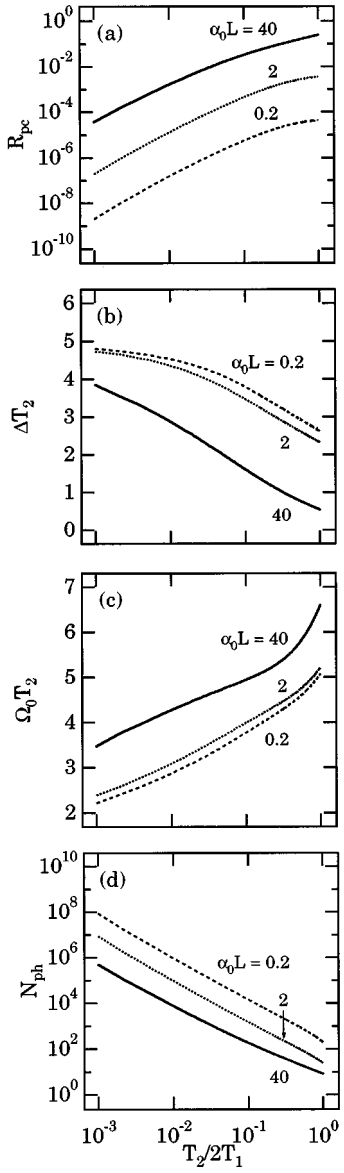

FIG. 2. Results of maximizing the reflectivity R_{pc} for $\alpha_0 L=0.2$, 2, and 40 while holding the probe-pump detuning fixed at $\delta_s T_2=5$. (a) Maximum R_{pc} vs $T_2/2T_1$. (b) The pump-resonance detuning ΔT_2 vs $T_2/2T_1$ that produces the maximum R_{pc} shown in (a). (c) Pump-field strength $\Omega_0 T_2$ vs $T_2/2T_1$ that produces the maximum R_{pc} shown in (a). (d) The photon noise factor N_{ph} vs $T_2/2T_1$ for the conditions giving the maximized R_{pc} of (a).

fluctuations in the medium and lowers the maximum achievable reflectivity [as shown in Fig. 2(a)]. Thus, the presence of collisions always causes the PCM to operate farther from the ideal quantum-noise limit. We also see that increasing $\alpha_0 L$ at fixed T_2/T_1 causes the PCM to operate relatively closer to the ideal quantum-noise limit [Fig. 2(d)], which indicates that the maximum reflectivity grows faster than the corresponding excess noise as $\alpha_0 L$ increases. Pump absorption may begin to play an important role at larger values of the absorption path length.

We next consider the behavior of the system as a function of the pump-resonance detuning ΔT_2 for three values of the decay-time ratio T_2/T_1 (Fig. 3). In all cases, $\alpha_0 L=40$, $\delta_s T_2=5$, and the pump strength is chosen to be approxi-

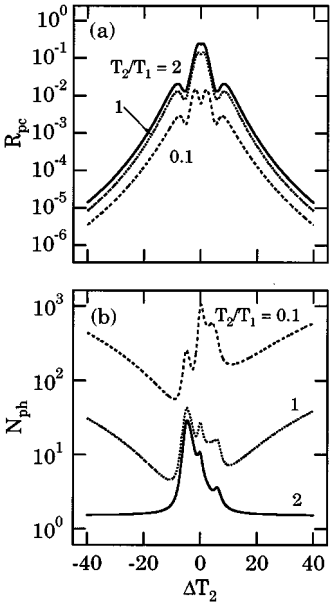

FIG. 3. The behavior of R_{pc} and N_{ph} as functions of pump-resonance detuning ΔT_2. Curves are shown for $T_2/T_1=2$, 1, and 0.1. All curves are for $\alpha_0 L=40$ and $\delta_s T_2=5$. For each value of T_2/T_1, the pump strength is fixed at its optimum value from Fig. 2: $\Omega_0 T_2=7$ for $T_2/T_1=2$, $\Omega_0 T_2=6$ for $T_2/T_1=1$, $\Omega_0 T_2=5$ for $T_2/T_1=0.1$. (a) R_{pc} vs ΔT_2. (b) N_{ph} vs ΔT_2. For $T_2/T_1=2$, $N_{ph}\rightarrow 1$ as $|\Delta T_2|$ increases while for $T_2/T_1<2$, N_{ph} reaches a minimum and then increases as $|\Delta T_2|$ increases.

mately equal to the optimum pump strength given in Fig. 2(c). Thus $\Omega_0 T_2=7$ for $T_2/T_1=2$, $\Omega_0 T_2=6$ for $T_2/T_1=1$, and $\Omega_0 T_2=5$ for $T_2/T_1=0.1$. Figure 3(a) shows the resulting reflectivity curves. The reflectivity has multiple peaks off resonance, with the maximum R_{pc} occurring for $|\Delta T_2|\sim 1$, where the best compromise is reached between the nonlinear gain and the absorption. Figure 3(b) shows the corresponding curves for the photon-noise factor. As the collision rate increases, the combination of the drop in the reflectivity [see Fig. 3(a)] and the increase in the excess noise results in larger values of N_{ph} at smaller values of T_2/T_1. For $T_2/T_1=2$, the quantum-noise limit is most closely approached ($N_{ph}\rightarrow 1$) by tuning far off resonance ($|\Delta T_2|\gg 1$), where the reflectivity is much less than maximum. In this case, the excess noise falls off faster than the reflectivity as the pump-resonance detuning increases. In the nonradiatively broadened limit, however, N_{ph} first reaches a minimum and then increases as $|\Delta T_2|$ increases. This change in behavior may be explained as follows: increasing the collision rate broadens the excess noise spectrum significantly while leaving the rate at which the reflectivity falls off with detuning relatively unchanged [see Fig. 3(a)]. Thus as more collisions are introduced, a point is reached where the excess noise falls off more slowly than the reflectivity, and N_{ph} then increases as $|\Delta T_2|$ increases at large detunings. The photon noise factor reaches its absolute minimum at approximately the same detuning that produces the farthest-off-resonance peaks in the reflectivity curve of Fig. 3(a), rather than at the detuning which gives the maximum reflectivity. The detuning that minimizes N_{ph} achieves the best compromise between the increase in the reflectivity as one tunes the pump

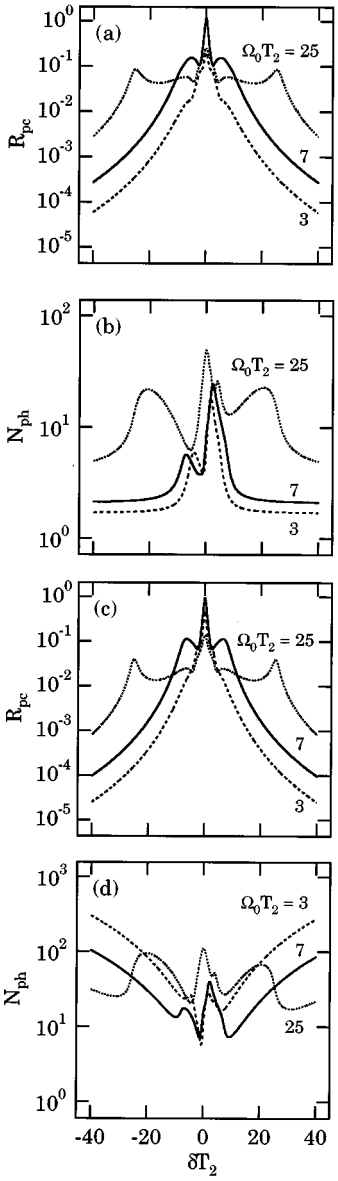

FIG. 4. Curves of R_{pc} and N_{ph} as functions of $\delta_s T_2$ for $\Omega_0 T_2=3$, 7, and 25. In all cases $\alpha_0 L=40$. The pump strengths are chosen to be less than, approximately equal to, and greater than the pump strength that maximizes R_{pc} at $\delta_s T_2=0$, given $\alpha_0 L$ and T_2/T_1. The values of ΔT_2 are selected to give approximately the best possible reflectivity after all the other parameters are fixed. Thus $\Delta T_2=-1$ for $\Omega_0 T_2=3$, $\Delta T_2=-2$ for $\Omega_0 T_2=7$, and $\Delta T_2=-4$ for $\Omega_0 T_2=25$. (a) R_{pc} vs $\delta_s T_2$ for $T_2/T_1=2$. (b) Curves of N_{ph} vs $\delta_s T_2$ for $T_2/T_1=2$ corresponding to the reflectivity curves in (a). (c) R_{pc} vs $\delta_s T_2$ for $T_2/T_1=1$. (d) Curves of N_{ph} vs $\delta_s T_2$ for $T_2/T_1=1$ corresponding to the reflectivity curves in (c).

frequency closer to the atomic resonance and the increase in the excess noise resulting from the resonant scattering of the pump fields.

Finally, we consider the behavior of the system as a function of the probe-pump detuning δT_2 for several values of the pump-field strength $\Omega_0 T_2$ (Fig. 4). In Figures 4(a) and 4(b), we fix $T_2/T_1=2$, $\alpha_0 L=40$, and $\Delta T_2=-1$ for $\Omega_0 T_2=3$, $\Delta T_2=-2$ for $\Omega_0 T_2=7$, and $\Delta T_2=-4$ for $\Omega_0 T_2=25$. Given T_2/T_1 and $\alpha_0 L$, the maximum reflectivity

at $\delta_s T_2 = 0$ is achieved for $\Omega_0 T_2 = 7$ and $\Delta T_2 = -2$. The other two pump strengths are chosen to be less than ($\Omega_0 T_2 = 3$) and greater than ($\Omega_0 T_2 = 25$) the optimum pump strength, and the corresponding pump-resonance detunings give the best possible reflectivity at $\delta_s T_2 = 0$ after the pump strength is fixed. Figure 4(a) shows that the reflectivity has peaks at $\delta_s T_2 = 0$ and at the Rabi sidebands. The effect of saturation can be seen for $\Omega_0 T_2 = 25$; the peak reflectivity decreases but the width of the reflectivity curve increases. Figure 4(b) shows the corresponding photon-noise factor curves. Except for small changes in the pump strength when δT_2 is near a reflectivity peak, lowering the reflectivity by weakening the pump fields at a fixed probe-pump detuning allows operation closer to the quantum-noise limit. Furthermore, $N_{ph} \rightarrow 1$ as $|\delta_s T_2|$ increases beyond $\sim |\delta_{Rabi} T_2|$, so in the radiatively broadened regime the excess noise falls off faster than the reflectivity as the pump fields are weakened and as the probe-pump detuning increases beyond $|\delta_{Rabi} T_2|$. Figures 4(c) and 4(d) show curves for the same parameter values shown in Figs. 4(a) and 4(b) except that here $T_2/T_1 = 1$. We see that in the nonradiatively broadened case, the broadening of the excess noise spectrum again causes the photon-noise factor to increase with probe-pump detuning when $|\delta_s T_2| \gtrsim |\delta_{Rabi} T_2|$. Thus N_{ph} is minimized at a given pump strength for probe-pump detunings approximately equal to those that produce the reflectivity peaks in Fig. 4(c).

IV. CONCLUSIONS

Our results for the noise spectrum of the conjugate beam lead to several conclusions. First, a radiatively broadened PCM operates close to the quantum-noise limit for large pump-resonance and signal-pump detunings, and at pump-field strengths such that the atoms are very weakly saturated. In this case, the excess noise produced by the PCM falls off faster than the reflectivity of the mirror as the nonlinearity decreases, which signifies that the reflectivity of the nearly quantum-noise limited PCM will be relatively small compared to that which would be obtained at larger pump strengths and smaller detunings (all other parameters remaining fixed). These results are in agreement with the conditions predicted in previous works for optimum squeezing via four-wave mixing in two-level systems [34–36]. In the collisionally broadened regime, operation closest to the ideal quantum-noise limit is achieved under conditions close to those that yield the maximum reflectivity. In this case, the excess noise falls off more slowly than does the reflectivity when the nonlinearity is too weak. These results are in qualitative agreement with recent experimental studies [40,41].

ACKNOWLEDGMENTS

This work was supported by the Office of Naval Research through Grant No. N00014-93-0538 and by the National Science Foundation through Grant No. PHY-9307511. G.S.A. thanks NSF Grant No. INT 9100685 for supporting this collaboration.

APPENDIX A: EXPRESSIONS FOR THE PROPAGATION COEFFICIENTS

This Appendix gives the explicit forms of the propagation coefficients α and κ. See Ref. [45] for the full derivation. In matrix form, the optical Bloch equations governing the polarization of the two-level atoms are

$$\frac{\partial \Phi}{\partial \tau} = A\Phi + I, \tag{A1}$$

where $\tau = t/T_2$, $\Phi_1 = \langle \hat{S}^+ \rangle$, $\Phi_2 = \Phi_1^*$, $\Phi_3 = \langle \hat{S}^z \rangle$, $I_1 = I_2 = 0$, and $I_3 = -T_2/2T_1$. The matrix A is given by

$$A = \begin{bmatrix} -(1 + i\Delta T_2) & 0 & i\Omega^* T_2 \\ 0 & -(1 - i\Delta T_2) & -i\Omega T_2 \\ i\Omega T_2/2 & -i\Omega^* T_2/2 & -T_2/T_1 \end{bmatrix}. \tag{A2}$$

Here $\Omega = \Omega_0 \cos(\mathbf{k} \cdot \mathbf{r})$ is the on-resonance Rabi frequency for the total pump field, $\Omega_0 = 4\mu |\mathbf{A}_p|/\hbar$, and $\Delta = \omega - \omega_0$ is the detuning of the pump field from the atomic resonance. By introducing the matrices

$$A^+ = \begin{bmatrix} 0 & 0 & 0 \\ 0 & 0 & -i\Omega T_2 \\ i\Omega T_2/2 & 0 & 0 \end{bmatrix} \tag{A3}$$

and

$$A^- = \begin{bmatrix} 0 & 0 & i\Omega^* T_2 \\ 0 & 0 & 0 \\ 0 & -i\Omega^* T_2/2 & 0 \end{bmatrix}, \tag{A4}$$

and by defining

$$K^+(\delta_s) = \sum_{jl} (i\delta_s T_2 + A)^{-1}_{2j} (A^+)_{jl} (A^{-1} I)_l \tag{A5}$$

and

$$K^-(\delta_s) = -\sum_{jl} (i\delta_s T_2 - A)^{-1}_{2j} (A^-)_{jl} (A^{-1} I)_l, \tag{A6}$$

the propagation coefficients may be expressed as

$$\alpha_1 = \frac{i\alpha_0}{2} K^+(\delta_s), \tag{A7}$$

$$\alpha_2 = -\frac{i\alpha_0}{2} [K^+(-\delta_s)]^*, \tag{A8}$$

$$i\kappa_1^* = \frac{i\alpha_0}{2} K^-(\delta_s), \tag{A9}$$

and

$$i\kappa_2 = \frac{i\alpha_0}{2} [K^-(-\delta_s)]^*, \tag{A10}$$

where $\delta_s = \omega_s - \omega$ is the probe-pump detuning, $\alpha_0 = 4\pi\mu^2 N \omega T_2/\hbar c$ is the small-signal, line-center absorp-

tion coefficient, and N is the number density of atoms. The ratio of the spontaneous emission time to the dephasing time is defined as $\Gamma = T_1/T_2$. The following definitions are made to condense the explicit expressions for the propagation coefficients:

$$\sigma = 1 + (\Delta T_2)^2, \tag{A11}$$

$$\gamma_1 = (\Gamma \delta_s T_2 + i)(\delta_s T_2 + \Delta T_2 + i)(\delta_s T_2 - \Delta T_2 + i), \tag{A12}$$

$$\xi_1 = -(\delta_s T_2 + i), \tag{A13}$$

$$\beta_1' = -\tfrac{1}{4}\alpha_0 \Gamma (\Omega_0 T_2)^2 (\Delta T_2 + i)\delta_s T_2, \tag{A14}$$

$$\beta_1 = 2\alpha_0 \sigma (\Gamma \delta_s T_2 + i)(\delta_s T_2 - \Delta T_2 + i), \tag{A15}$$

$$\zeta_1 = -\tfrac{1}{4}\alpha_0 \sigma \Gamma (\Omega_0 T_2)^2 \frac{\delta_s T_2 + 2i}{\Delta T_2 + i}, \tag{A16}$$

$$D_1 = \sigma\gamma_1 \left\{ \left(1 + \frac{\Gamma(\Omega_0 T_2)^2}{\sigma} \right)^{1/2} \left(1 + \frac{\Gamma \xi_1 (\Omega_0 T_2)^2}{\gamma_1} \right)^{1/2} \times \left[\left(1 + \frac{\Gamma(\Omega_0 T_2)^2}{\sigma} \right)^{1/2} + \left(1 + \frac{\Gamma \xi_1 (\Omega_0 T_2)^2}{\gamma_1} \right)^{1/2} \right] \right\}, \tag{A17}$$

and

$$N_1 = \frac{\sigma \xi_1 \Gamma (\Omega_0 T_2)^2 \left(1 + \frac{\Gamma(\Omega_0 T_2)^2}{\sigma} \right)^{1/2} - \gamma_1 \Gamma (\Omega_0 T_2)^2 \left(1 + \frac{\xi_1 \Gamma (\Omega_0 T_2)^2}{\gamma_1} \right)^{1/2}}{4\gamma_1 \sigma \left[\left(1 + \frac{\xi_1 \Gamma (\Omega_0 T_2)^2}{\gamma_1} \right)^{1/2} - \left(1 + \frac{\Gamma(\Omega_0 T_2)^2}{\sigma} \right)^{1/2} \right]}. \tag{A18}$$

The quantities γ_2, ξ_2, β_2', β_2, ζ_2, D_2, and N_2 are obtained from the corresponding expressions above by making the replacement $\delta_s \rightarrow -\delta_s$ and taking the complex conjugate, for example, $\gamma_2(\delta_s) = \gamma_1^*(-\delta_s)$. In terms of the quantities above, the propagation coefficients may be written as

$$\alpha_1 = \frac{\beta_1 N_1 + \beta_1'}{iD_1}, \tag{A19}$$

$$\alpha_2 = -\frac{\beta_2 N_2 + \beta_2'}{iD_2}, \tag{A20}$$

$$i\kappa_1^* = -\frac{\zeta_1}{iD_1}, \tag{A21}$$

and

$$i\kappa_2 = -\frac{\zeta_2}{iD_2}. \tag{A22}$$

To obtain these coefficients, an average over a spatial period of the grating formed by the pump waves is performed to eliminate non-phase-matched terms, and the wave-vector mismatch associated with the four-wave mixing interaction coupling the signal and conjugate fields is neglected.

APPENDIX B: CALCULATION OF THE CORRELATION FUNCTIONS

This Appendix summarizes the calculation of the correlation functions (2.14a)–(2.14c). In matrix form, the Bloch equations are

$$\frac{\partial \Phi}{\partial \tau} = A\Phi + I, \tag{B1}$$

as discussed at the begining of Appendix A. The quantum regression theorem allows the evaluation of all correlation functions in terms of the steady-state solutions to Eq. (B1), which are given by

$$\Phi_1 = -\frac{\Omega^* T_2 (i + \Delta T_2)}{2D(0)} \frac{T_2}{T_1}, \tag{B2}$$

$$\Phi_2 = -\frac{\Omega T_2 (-i + \Delta T_2)}{2D(0)} \frac{T_2}{T_1}, \tag{B3}$$

and

$$\Phi_3 = -\frac{1 + (\Delta T_2)^2}{2D(0)} \frac{T_2}{T_1}, \tag{B4}$$

where $D(\delta_s)$ is given by

$$D(\delta_s) = \det(U) = \left(\frac{T_2}{T_1} + i\delta_s T_2 \right) [(1 + i\delta_s T_2)^2 + (\Delta T_2)^2] + (1 + i\delta_s T_2)|\Omega T_2|^2. \tag{B5}$$

The matrix $U = (i\delta_s T_2 - A)^{-1}$ is given by

$$U=\frac{1}{D(\delta_s)}\begin{bmatrix}[1+i(\delta_s-\Delta)T_2](T_2/T_1+i\delta_s T_2)+|\Omega T_2|^2/2 & (\Omega T_2)^2/2 & -\Omega T_2[(\delta_s-\Delta)T_2-i]/2 \\ (\Omega^* T_2)^2/2 & [1+i(\delta_s+\Delta)T_2][T_2/T_1+i\delta_s T_2]+|\Omega T_2|^2/2 & \Omega^* T_2[(\delta_s+\Delta)T_2-i]/2 \\ -\Omega^* T_2[(\delta_s-\Delta)T_2-i] & \Omega T_2[(\delta_s+\Delta)T_2-i] & [(1+i\delta_s T_2)^2+(\Delta T_2)^2]\end{bmatrix} \tag{B6}$$

By introducing the matrix $V=U(\delta_s\rightarrow-\delta_s)$ and the two vectors

$$\psi=\begin{bmatrix}\frac{1}{2}-\Phi_3-\Phi_2\Phi_1 \\ -\Phi_2\Phi_2 \\ \frac{1}{2}\Phi_2-\Phi_2\Phi_3\end{bmatrix} \tag{B7}$$

and

$$\Lambda=\begin{bmatrix}\frac{1}{2}+\Phi_3-\Phi_2\Phi_1 \\ -\Phi_2\Phi_2 \\ -\frac{1}{2}\Phi_2-\Phi_2\Phi_3\end{bmatrix}, \tag{B8}$$

the correlation functions can be expressed as

$$\tilde{X}^{-+}(\delta_s)=2\ \mathrm{Re}\left[\sum_j U_{1j}\psi_j\right], \tag{B9}$$

$$\tilde{X}^{+-}(\delta_s)=2\ \mathrm{Re}\left[\sum_j V_{1j}\Lambda_j\right], \tag{B10}$$

and

$$\tilde{X}^{++}(\delta_s)=\sum_j [V_{2j}\Lambda_j+U_{2j}\psi_j]^*. \tag{B11}$$

In Eqs. (B9)–(B11), the right-hand side is averaged over a spatial period of the grating formed by the pump waves to eliminate non-phase-matched terms.

[1] *Optical Phase Conjugation*, edited by R. A. Fisher (Academic, New York, 1983).
[2] B. Y. Zel'dovich, N. F. Pilipetsky, and V. V. Shkunov, *Principles of Phase Conjugation* (Springer-Verlag, Berlin, 1985).
[3] L. Petersen, U. Gliese, and T. N. Nielsen, IEEE J. Quantum Electron. **QE-30**, 2526 (1994).
[4] R. M. Jopson, A. H. Gnauck, and R. M. Derosier, Electron. Lett. **29**, 526 (1993).
[5] M. C. Tatham, G. Sherlock, and L. D. Westbrook, Electron. Lett. **29**, 1851 (1993).
[6] W. Pieper, C. Kurtzke, R. Schnabel, D. Breuer, R. Ludwig, K. Petermann, and H. G. Weber, Electron. Lett. **30**, 724 (1994).
[7] C. M. Caves, Phys. Rev. D **26**, 1817 (1982).
[8] Y. Yamamoto and H. A. Haus, Rev. Mod. Phys. **58**, 1001 (1986).
[9] A. L. Gaeta and R. W. Boyd, Phys. Rev. Lett. **60**, 2618 (1988).
[10] J. Bajer and J. Perina, Opt. Commun. **85**, 261 (1991).
[11] See, for example, P. W. Milonni, E. J. Bochove, and R. J. Cook, J. Opt. Soc. Am. B **6**, 1932 (1989); P. W. Milonni, E. J. Bochove, and R. J. Cook, Phys. Rev. A **40**, 4100 (1989).
[12] J. R. R. Leite, P. Simoneau, D. Bloch, S. Le Boiteux, and M. Ducloy, Euophys. Lett. **2**, 747 (1986).
[13] M. Vallet, M. Pinard, and G. Grynberg, Opt. Commun. **81**, 403 (1991).
[14] J. Nilsen, N. Gluck, and A. Yariv, Opt. Lett. **6**, 554 (1981).
[15] D. G. Steel and R. C. Lind, Opt. Lett. **6**, 554 (1981).
[16] P. R. Hemmer, D. P. Katz, J. Donoghue, M. Cronin-Golomb, M. S. Shahriar, and P. Kumar, Opt. Lett. **20**, 982 (1995).
[17] D. S. Glassner and R. J. Knize, Phys. Rev. Lett. **74**, 2212 (1995).
[18] V. Vieux, P. Gravey, N. Wolffer, and G. Picoli, Appl. Phys. Lett. **58**, 2880 (1991).
[19] J. Feinberg and R. W. Hellwarth, Opt. Lett. **5**, 519 (1980); **6**, 257 (1981).
[20] D. M. Pepper, Appl. Phys. Lett. **49**, 1001 (1986).
[21] V. I. Bespalov, A. Z. Matveev, and G. A. Pasmanik, Radiophys. Quantum Electron. **29**, 818 (1987); N. F. Andreev *et al.* Rev. Roum. Phys. **31**, 951 (1986).
[22] N. F. Andreev, V. I. Bespalov, M. A. Dvoretsky, and G. A. Pasmanik, IEEE J. Quantum Electron. **QE-25**, 346 (1989).
[23] K. D. Ridley and A. M. Scott, Opt. Lett. **15**, 777 (1990).
[24] M. Lucente, G. M. Carter, and J. G. Fujimoto, Appl. Phys. Lett. **53**, 467 (1988).
[25] H. P. Yuen and J. H. Shapiro, Opt. Lett. **4**, 334 (1979).
[26] J. Jansky and Yu. Ya. Yushin, Opt. Commun. **49**, 290 (1984).
[27] B. Yurke, Phys. Rev. A **32**, 300 (1985).
[28] R. S. Bondurant, P. Kumar, J. H. Shapiro, and M. Maeda, Phys. Rev. A **30**, 343 (1984).
[29] G. J. Milburn, D. F. Walls, and M. D. Levenson, J. Opt. Soc. Am. B **1**, 390 (1984).
[30] G. S. Agarwal, Phys. Rev. A **34**, 4055 (1986).
[31] M. Sargent III, D. A. Holm, and M. S. Zubairy, Phys. Rev. A **31**, 3112 (1985).
[32] G. S. Agarwal and R. W. Boyd, Phys. Rev. A **38**, 4019 (1988).
[33] M. D. Levenson, R. M. Shelby, A. Aspect, M. Reid, and D. F. Walls, Phys. Rev. A **32**, 1550 (1985).
[34] M. D. Reid and D. F. Walls, Phys. Rev. A **31**, 1622 (1985).

[35] M. D. Reid and D. F. Walls, Opt. Commun. **50**, 406 (1984).
[36] M. D. Reid and D. F. Walls, Phys. Rev. A **34**, 4929 (1986).
[37] S. -T. Ho, P. Kumar, and J. H. Shapiro, Phys. Rev. A **37**, 2017 (1988); S.-T. Ho, P. Kumar, and J. H. Shapiro, J. Opt. Soc. Am. B **8**, 37 (1991).
[38] R. E. Slusher, L. W. Hollberg, B. Yurke, J. C. Mertz, and J. F. Valley, Phys. Rev. Lett. **55**, 2409 (1985); R. E. Slusher, L. W. Hollberg, B. Yurke, J. C. Mertz, and J. F. Valley, Phys. Rev. A **31**, 3512 (1985).
[39] R. M. Shelby, M. D. Levenson, S. H. Perlmutter, R. G. DeVoe, and D. F. Walls, Phys. Rev. Lett. **57**, 691 (1986).
[40] M. Y. Lanzerotti, R. W. Schirmer, and A. L. Gaeta, Appl. Phys. Lett. **69**, 1199 (1996).
[41] M. Y. Lanzerotti, R. W. Schirmer, A. L. Gaeta, and G. S. Agarwal, Phys. Rev. Lett. **77**, 2202 (1996).
[42] A. L. Gaeta, R. W. Boyd, and G. S. Agarwal, Phys. Rev. A **46**, 4271 (1992).
[43] A. Rosenhouse-Dantsker, A. D. Wilson-Gordon, and H. Friedmann, Phys. Rev. A **52**, 4839 (1995).
[44] W. V. Davis, M. Kauranen, E. M. Nagasako, R. J. Gehr, A. L. Gaeta, R. W. Boyd, and G. S. Agarwal, Phys. Rev. A **51**, 4152 (1995).
[45] D. J. Harter and R. W. Boyd, IEEE J. Quantum Electron. **QE-16**, 1126 (1980).